Development of a pure diffusion quantum Monte Carlo method using a full generalized Feynman–Kac formula. II. Applications to simple systems

Michel Caffarel and Pierre Claverie
Dynamique des Interactions Moléculaires, Université Pierre et Marie Curie, Paris VI, Tour 22, 4 Place Jussieu, 75252 Paris, Cedex 05, France.

(Received 26 January 1987; accepted 15 September 1987)

We have described in part I of this work the theoretical basis of a quantum Monte Carlo method based on the use of a pure diffusion process and of the so-called full generalized Feynman–Kac (FGFK) formula. In this second part, we present a set of applications (one-dimensional oscillator, helium-like systems, hydrogen molecule) with the purpose of illustrating in a systematic way the various aspects pertaining to the practical implementation of this method. We thus show how energy and other observables can be obtained, and we discuss the various sources of biases occurring in the different procedures (notably the so-called short-time approximation pertaining to the generation of the sample trajectories of the diffusion process, and the numerical integration pertaining to the evaluation of the "Feynman–Kac factor"). After having thus considered the case of the genuine "bosonic" ground state, we illustrate the various proposals for dealing with some "relative" ground state (namely the lowest state belonging to some prescribed symmetry), one of the most important cases being obviously the physical ground state of many-fermion systems (owing to the Pauli principle requirements). More specifically, we consider the so-called fixed-node approximation (FNA), on one hand, and two variants of a potentially exact procedure, the so-called simple projection (SP) and release-node projection (RNP) methods, on the other hand. Finally, some perspectives concerning future developments are outlined.

I. INTRODUCTION

In paper I,[1] we have shown how quantum mechanical properties can be expressed in terms of functional integrals using our full generalized Feynman–Kac (FGFK) formula. More precisely, these functional integrals involve in their integrand the operators corresponding to the desired observables, and make use of the functional measure corresponding to a *pure diffusion* process, which is itself associated in a simple way with some reference function denoted $\varphi_0^{(0)}$.

When $\varphi_0^{(0)}$ is chosen to be square integrable (which is always the case in our applications), this associated diffusion process is ergodic (recurrent, actually), and accordingly the functional integrals may be rigorously expressed as time-averages along any single sample trajectory (or any finite number of sample trajectories) of the process. From the practical point of view, this feature sharply contrasts with the situation encountered when dealing with the Feynman path integral (in imaginary time) or the Wiener integral (involved in the usual Feynman–Kac formula). Indeed, in the two latter cases, no ergodic property holds, and consequently the numerical evaluation of the functional integrals would require summing over an unlimited number of trajectories.

As concerns the generation of the trajectories themselves, we use the Langevin equation associated with the diffusion process, with a suitable time discretization. In earlier stages of our work, we contented ourselves with a constant time step, but later on we were led to improve our procedure by using a variable time step, noticeably for avoiding so-called "overshooting" effects (see e.g., Ref. 2) near hypersurfaces where the drift vector of the Langevin equation becomes infinite.

An important problem consists in evaluating quantities pertaining to the lowest state belonging to some prescribed symmetry type, rather than the "absolute" lowest state only. Perhaps the most important special case is that of N-fermion systems (with $N>2$), since the Pauli principle requires that the physical states belong to some *restricted* set of representations of the permutation group, thereby excluding the absolute (bosonic) ground state, which belongs to the (fully symmetric) identity representation. In order to illustrate the various possibilities of treating this problem, we put into application the three procedures examined in part I, namely the simple projection (SP) method, the fixed-node approach (FNA), and the release-node projection (RNP) method.

The contents of the paper are as follows. In sec. II, we consider several one-dimensional problems of increasing complexity with the purpose of illustrating in a stepwise way the essential properties of the method and its different versions. More specifically, we consider first (Sec. II A) for $H^{(0)}$ a harmonic oscillator Hamiltonian and we take $H = H^{(0)}$ (i.e., $V_p = 0$); this case will enable us to check some basic features of the algorithms (noticeably the so-called short-time approximation). Then (Sec. II B), using the same $H^{(0)}$ but now $V_p = x^2$ (so that H is still harmonic), we can study the error due to the numerical integration of the "Feynman–Kac factor" $\exp\{-\int V_p[X(s)]ds\}$. In Sec. II C, we consider as total Hamiltonian: $H = -\frac{1}{2}d^2/dx^2 + \frac{1}{2}x^2 + x^4$, but we now study successively *two* choices for $\varphi_0^{(0)}$, from which we build two different reference Hamiltonian $H^{(0)}$'s, with corresponding potential V_p's having qualitatively different magnitudes (varying like x^4 or x^2, respectively for $|x| \to +\infty$). We also introduce here the use of the Padé–integral transform for extracting the first excitation energies from a set of sampled values of $I(t)$, the matrix element of the "evolution

 0021-9606/88/021100-10$02.10

operator" (in imaginary time) $\exp(-tH)$. In Sec. II D we consider (for the same Hamiltonian H as in Sec. II C) the problem of obtaining the lowest state of some *prescribed symmetry* (odd parity here) different from the one of the genuine ground state (even parity here). For that purpose, we introduce the simple projection (SP) method and the fixed-node approximation (FNA), which turns out to be exact in this case. Finally, in Sec. II E we return to the harmonic oscillator Hamiltonian, but we now focus our attention on the *second* excited state φ_2, whose "peculiar nodes" are *not* imposed by any symmetry (see part I). We can then study a genuine case of fixed-node *approximation*, and also the release-node projection (RNP) method for reaching the exact result. It must be emphasized that the cases treated in Secs. II D and II E illustrate the methods which will be necessary for dealing with the N-fermion systems ($N>2$). In Sec. III, we describe our first applications to the simplest atomic and molecular systems. In Sec. III A we deal with bosonic ground state properties (*energies* and *mean values of other observables*) for two-electron systems: helium atom and helium-like ions and the hydrogen molecule. These cases enable us to illustrate efficient choices of $\varphi_0^{(0)}$ (from which result nontrivial $H^{(0)}$ and V_p operators). In Sec. III B, we consider, as a preliminary step towards the study of N-fermion systems, the problem of obtaining the energy of the lowest helium triplet, both with the simple projection and fixed-node approach (which can still be made exact here). Finally we present in Sec. IV some perspectives about the treatment of larger systems, concerning the evaluation of energies, mean values of other observables, and response properties.

II. ONE-DIMENSIONAL SYSTEMS

A. Harmonic oscillator

The Hamiltonian is written

$$H = -\frac{1}{2}\frac{d^2}{dx^2} + \frac{1}{2}x^2. \tag{2.1}$$

According to the general theory presented in part I, the Hamiltonian is decomposed into two parts:

$$H = H^{(0)} + V_p, \tag{2.2}$$

where $H^{(0)}$ is the so-called reference Hamiltonian built from a given reference function $\varphi_0^{(0)}$ and V_p the perturbing potential defined as the difference $H - H^{(0)}$. In this simple case, the reference function may be chosen as the exact ground state φ_0 of H, namely

$$\varphi_0^{(0)}(x) = \varphi_0(x) = e^{-x^2/2}. \tag{2.3}$$

The perturbing potential V_p which is expressed in terms of the reference function as [see Eq. (3.2) of part I]

$$V_p = V - E_0^{(0)} - \tfrac{1}{2}\nabla^2\varphi_0^{(0)}/\varphi_0^{(0)}, \tag{2.4}$$

where V is the potential energy of H and $E_0^{(0)}$ an arbitrary constant, becomes here

$$V_p = 1/2 - E_0^{(0)}. \tag{2.5}$$

Note that the arbitrary reference energy $E_0^{(0)}$ may be chosen so that $V_p = 0$.

Now, the full generalized Feynman–Kac (FGFK) formula permits to express the following matrix element of the (imaginary-time) evolution operator $\exp(-tH)$:

$$I(t) = \langle f\varphi_0^{(0)} | e^{-t(H - E_0^{(0)})} | g\varphi_0^{(0)} \rangle \tag{2.6}$$

as a functional integral [see Eq. (4.1) of part I]. Using the ergodic property of the reference diffusion process built from $\varphi_0^{(0)}$ [cf. Eq. (3.15) of part I], this functional integral may be expressed as a time-average over the stochastic trajectories of this process. In the present case where $V_p = 0$, we obtain

$$I(t) = \lim_{T\to+\infty} \frac{1}{T}\int_0^T f[X^{(0)}(-t/2+\tau)] \times g[X^{(0)}(t/2+\tau)]\,d\tau, \tag{2.7}$$

where $X^{(0)}(s)$ denotes an arbitrary trajectory of the reference diffusion process. It must be pointed out that the ergodic property may be invoked here since $\varphi_0^{(0)}$ has been chosen square integrable (cf. Sec. III of part I).

On the other hand, using the well-known equality

$$\varphi_n(n) = \varphi_0(n)(2^n n!)^{-1/2} H_n(x), \tag{2.8}$$

where $H_n(x)$ are the Hermite polynomials, and choosing the functions f and g as follows

$$f(x) = g(x) = (2^n n!)^{-1/2} H_n(x), \tag{2.9}$$

the matrix element [Eq. (2.6)] takes on the simpler form

$$I(t) = e^{-t(E_n - E_0^{(0)})} \tag{2.10}$$

and from Eqs. (2.10) and (2.7) we obtain the basic equality

$$e^{-t(E_n - E_0^{(0)})} = \lim_{T\to+\infty} \frac{1}{T}\int_0^T \frac{1}{2^n n!} H_n[X^{(0)}(-t/2+\tau)] \times H_n[X^{(0)}(t/2+\tau)]\,d\tau. \tag{2.11}$$

Then, by evaluating numerically the right-hand side of Eq. (2.11) above, the excited energies of the system can be calculated.

As concerns the construction of the arbitrary stochastic trajectory $X^{(0)}(s)$, a discretized form of the stochastic differential equation (SDE), suitable for computer simulation, is introduced (see e.g., Ref. 3, Sec. 3.6)

$$X(t+\Delta t) = X(t) + b[X(t)]\Delta t + (\Delta t)^{1/2}\eta, \tag{2.12}$$

where the η's denote successive samples of a Gaussian random variable with zero mean and variance 1. The drift function $b(x)$ above may be evaluated from the general expression of the drift vector given in terms of the reference function [see Eq. (2.11a) of part I]:

$$\mathbf{b} = \nabla\varphi_0^{(0)}/\varphi_0^{(0)}. \tag{2.13}$$

Using expression (2.3) for the reference function, we obtain

$$b(x) = -x. \tag{2.14}$$

As a second step, the numerical integration involved in the right-hand side of Eq. (2.11) is performed over the stochastic trajectory $X^{(0)}(s)$ for large but finite T. In fact, by using a suitable updating scheme, the two operations (construction of the trajectory and integration) are performed simultaneously.

The numerical realization has put three points into evi-

dence: (1) The pseudorandom generator used for generating Gaussian numbers must have a very good quality in order to prevent the apparition of biases and artificial oscillations in the results. (2) The statistical fluctuations are significantly decreased when a large number of trajectories starting from points distributed according to the stationary probability density $p^{(0)}(x)=\varphi_0^{(0)2}$ are used, rather than a single one only. Furthermore, by decomposing this set of trajectories into a few subsets (typically about ten) and by evaluating the functional integral *independently* for each of these subsets, it is possible to obtain an evaluation of the variance using standard statistical methods.[4] (3) Time-discretization of the SDE (with a time step Δt) introduces a systematic bias in the results: this is the well-known "short-time approximation" (see, e.g., Refs. 2 and 5). More precisely, by using the discretized form [Eq. (2.12)] of the SDE, the exact transition probability density $p^{(0)}(x]y,\Delta t)$ corresponding to the exact continuous form of the SDE is approximated by the following transition density:

$$P^{(0)}_{\text{approx}}(x]y,\Delta t) = (2\pi\Delta t)^{-1/2}\exp\{-[y-x-b(x)\Delta t]^2/2\Delta t\}. \tag{2.15}$$

In the particular case of the diffusion process associated with the Gaussian reference function (2.3) (the so-called "Ornstein–Uhlenbeck" process) $p^{(0)}(x]y,\Delta t)$ is exactly known (see e.g., Sec. 5.3 of Ref. 3):

$$P^{(0)}(x]y,\Delta t) = [\pi(1-\gamma^2)]^{-1/2} \times\exp[-(y-\gamma x)^2/(1-\gamma^2)], \tag{2.16}$$

where $\gamma=\exp(-\Delta t)$.

As it must be, the two expressions [Eqs. (2.15) and (2.16)] coincide when Δt goes to zero. Thus, in the special case under consideration, we can avoid the short-time approximation by generating the stochastic trajectories from the transition probability [Eq. (2.16)] instead of Eq. (2.15).

In Table I, results for some of the lowest excited energies are presented. Expressions (2.15) and (2.16), above, for the transition probability density have been used to generate trajectories. The bias resulting from the short-time approximation appears clearly. The improvement resulting from the removal of this approximation is clearly evidenced when using the *exact* transition probability density. As concerns the biased results, no procedure of extrapolation to $\Delta t=0$ has been used since the statistical fluctuations are of the same order of magnitude as the biases. Results for $\Delta t=0.01$ may be considered as satisfactory.

TABLE I. First excited energies for the harmonic oscillator.[a]

	E_1	E_2	E_3
	Biased results[b]		
$\Delta t=0.04$	1.518(7)	2.54(2.6)	3.58(6)
$\Delta t=0.03$	1.514(8)	2.53(3)	3.55(7.5)
$\Delta t=0.02$	1.510(9)	2.51(3.3)	3.51(11)
$\Delta t=0.01$	1.504(15)	2.50(5.4)	3.45(17)
	Nonbiased results[c]		
$\Delta t=0.04$	1.499(7)	2.50(2.6)	3.52(6)
	Exact results		
	1.5	2.5	3.5

[a] Calculations have been performed using 100 trajectories (divided in 10 subsets of 10 trajectories each for the purpose of evaluating the standard deviation, and hence the confidence interval corresponding to some prescribed level of accuracy). 500 000 elementary time steps have been used for each trajectory. Energies are derived from formula (2.11) with $t=0.4$. Statistical uncertainties (99% confidence interval) are indicated in parentheses.
[b] Using Eq. (2.15).
[c] Using Eq. (2.16).

B. Harmonic oscillator with a harmonic perturbation

The Hamiltonian is written

$$H=-\frac{1}{2}\frac{d^2}{dx^2}+\frac{1}{2}x^2+\lambda x^2. \tag{2.17}$$

The reference function and energy are chosen as follows

$$\varphi_0^{(0)}(x)=e^{-x^2/2}, \tag{2.18a}$$

$$E_0^{(0)}=\tfrac{1}{2}. \tag{2.18b}$$

Using Eqs. (2.4), (2.2), and (2.18), we thus obtain

$$H^{(0)}=-\frac{1}{2}\frac{d^2}{dx^2}+\frac{1}{2}x^2, \tag{2.19a}$$

$$V_p=\lambda x^2. \tag{2.19b}$$

In this example, we use a high-quality generator of pseudorandom numbers, a large number of trajectories (about 100) and the exact transition probability density (no short-time approximation). We are then in a position to test the numerical effectiveness of our generalized Feynman–Kac formula [Eq. (4.1) of part I] in a case where the perturbing potential V_p is not zero. Using as usual the ergodic property, the quantum matrix element (2.6) (with $f=g=1$) may be rewritten as

$$I(t)=\lim_{T\to+\infty}\frac{1}{T}\int_0^T\exp\left[-\int_{-t/2+\tau}^{t/2+\tau}V_p[X^{(0)}(s)]ds\right]d\tau. \tag{2.20}$$

Now, if we want to extract the ground state energy E_0 of H, the following formula valid for large but finite t could be used [see Eqs. (4.4) and (4.5) of part I]:

$$-\frac{1}{t}\log I(t) = E_0-E_0^{(0)}-\frac{1}{t}\log|\langle\varphi_0^{(0)}|\varphi_0\rangle|^2+O(e^{-t}). \tag{2.21}$$

In actual fact, the error $O(1/t)$ due to the second term may be very easily suppressed by considering the slope of $\log I(t)$ at infinity:

$$-[\log I(t_2)-\log I(t_1)]/(t_2-t_1) = E_0-E_0^{(0)}+O(e^{-t_1}) \quad t_2>t_1 \tag{2.22}$$

which now involves, for large t_2 and t_1, an exponentially small error.

On the other hand, using the eigensolutions for $H^{(0)}$ and H, that is, respectively,

$$\varphi_n^{(0)}(x)=\pi^{-1/4}(2^n n!)^{-1/2}H_n(x)e^{-x^2/2} \tag{2.23a}$$

$$E_n^{(0)}=n+1/2 \tag{2.23b}$$

and

$$\begin{cases}\varphi_n(x) = \omega^{1/4}\pi^{-1/4}(2^n n!)^{-1/2} H_n(\omega^{1/2}x)e^{-\omega x^2/2} & \text{with } \omega = (1+2\lambda)^{1/2} \quad (2.24a)\\ E_n = (n+1/2)\omega & (2.24b)\end{cases}$$

and inserting these expressions into the expanded expression for $I(t)$ in terms of the complete set of eigenstates of H given in Eq. (4.4) of part I, it is possible to obtain after a few algebric manipulations the analytical value of $I(t)$:

$$I(t) = \frac{2\omega^{1/2}}{1+\omega} e^{-t/2(\omega-1)} \times\left[1 + \sum_{n=1}^{+\infty} \frac{(2n-1)!!}{2^n n!}\left(\frac{\omega-1}{\omega+1}\right)^{2n} e^{-2\omega t n}\right]. \quad (2.25)$$

The numerical realization (with $\lambda = 1$, i.e., $\omega = 3^{1/2}$) shows the existence of a bias for $I(t)$ when $\Delta t = 0.2$ (see Table II). This bias is due to use of a finite Riemann sum for evaluating the integral $\int V_p\, ds$ appearing in Eq. (2.20). However, as we can see in Table II, it seems that this bias is very small compared with previous biases due to the short-time approximation.

C. Quartic oscillator. Evaluation of the ground state energy E_0

The Hamiltonian is written

$$H = -\frac{1}{2}\frac{d^2}{dx^2} + \frac{1}{2}x^2 + x^4. \quad (2.26)$$

In this example we illustrate a basic feature of the method namely, the importance of choosing a "good" reference function $\varphi_0^{(0)}$. As already noticed above, if $\varphi_0^{(0)}$ were chosen as the exact function φ_0, the perturbing potential defined by Eq. (2.4) would be zero ($E_0^{(0)}$ is arbitrary and may be chosen so that $V_p = 0$) and the variance would vanish. In the general case, the numerical experience has shown that the importance of the statistical fluctuations is directly related to the "importance" of this perturbing potential. Two cases have been treated here. In the first one, we make the natural choice:

$$\varphi_0^{(0)} = e^{-x^2/2} \quad (2.27)$$

which leads to

$$V_p = x^4 + \tfrac{1}{2} - E_0^{(0)}. \quad (2.28)$$

By contrast, in the second case, the behavior for $|x| \to +\infty$ of the exact eigenfunction φ_0 is incorporated into $\varphi_0^{(0)}$. The asymtotic form of φ_0 is easily deduced from the asymtotic form of the Schrödinger equation. We obtain:

$$\varphi_0(x) \underset{|x|\to+\infty}{\sim} e^{-2^{1/2}/3\,|x|^3}. \quad (2.29)$$

Consequently, our second choice will be

$$\varphi_0^{(0)}(x) = e^{-2^{1/2}/3\,|x|^3} \quad (2.30)$$

and from Eq. (2.4) above it then follows that

$$V_p = \tfrac{1}{2}x^2 + 2^{1/2}|x| - E_0^{(0)}. \quad (2.31)$$

With this choice, the quartic part of V_p has been removed. The ground state energy E_0 has been evaluated using the two forms for $\varphi_0^{(0)}$ and for different values of the time step Δt. Results are displayed in Table III. The important point is that with the expression (2.30) for $\varphi_0^{(0)}$, the variance is actually smaller than with the expression (2.27). From now on, this strategy of variance reduction will be systematically used.

From the expanded form [Eq. (4.4)] of part I it is clear that $I(t)$ may be written in the following form:

$$I(t) = \sum_i c_i e^{-\lambda_i t}. \quad (2.32)$$

TABLE II. Harmonic oscillator with a harmonic perturbation.[a]

	E_0
QMC ($\Delta t = 0.02$)	0.8660(14)
Exact[b]	0.86603
	$I(t=3)$
QMC:	
$\Delta t = 0.2$	0.3227(4)
$\Delta t = 0.1$	0.3214(4)
$\Delta t = 0.075$	0.3213(4)
Exact[c]	0.32131

[a] Calculations have been performed using 100 trajectories, 500 000 elementary time steps for each trajectory. Energy is derived from formula (2.22) with $t_2 = 9$ and $t_1 = 8$. Statistical uncertainties are indicated in parentheses.
[b] From formula (2.24b).
[c] Calculated from formula (2.25).

TABLE III. Ground state and second excited state energies for the quartic oscillator.

	E_0[a]	
First choice for $\varphi_0^{(0)}$[b]		
$\Delta t = 0.01$[c]	0.8037(20)	
Second choice for $\varphi_0^{(0)}$[d]		
$\Delta t = 0.1$	0.8199(5)	
$\Delta t = 0.075$	0.8156(6)	
$\Delta t = 0.05$	0.8114(7)	
$\Delta t = 0.025$	0.8079(8)	
Extrapolation[e]	0.8037(10)	
Exact[f]	0.80377	
	Excited energies[g]	
	E_0	E_2
QMC	0.8033(30)	5.18(2)
Exact[f]	0.80377	5.179

[a] Energy is derived from formula (2.22) with $t_2 = 4$ and $t_1 = 3$. Calculations have been performed using 1000 trajectories with 75 000 elementary time steps for each trajectory.
[b] Expression (2.27).
[c] Using Eq. (2.16).
[d] Expression (2.30).
[e] A least-squares fit to a straight line has been performed.
[f] Reference 15.
[g] A Padé z-transform analysis of $I(t)$ has been done with 40 regularly sampled values $I(t_i)$ with t_i ranging from 0 to 4. The calculation has been performed using 100 trajectories, 200 000 elementary time steps for each trajectory and $\Delta t = 0.1$.

The expression (2.22) enables us to extract the smallest exponant λ_0 using the behavior of $I(t)$ for large t. Now, we would like to extract more information about $I(t)$. More precisely, we are faced with the general problem of the analysis of functions expressed as sum of real exponentials. We used here the Padé-integral transform method recently developed.[6] This method enables us to evaluate excited energies. However, the main point appears to be the possibility to perform an analysis of $I(t)$ without using large values of t. The importance of such a possibility has been already emphasized in part I (Sec. VI C 2). A Padé-z transform analysis of $I(t)$ has been performed here. Results are displayed in Table III.

D. Quartic oscillator. Evaluation of the first excited energy E_1

The first excited energy E_1 of the quartic oscillator may be viewed as the ground state energy of the *odd* symmetry subspace. Since this subspace is *not* the symmetry subspace of the genuine ground state E_0, this example may be considered as a *model problem* for illustrating the constraints due to the Pauli principle requirements (see part I, Sec. VI). Two of the procedures designed for dealing with such a situation are presented here.

1. Simple projection (SP) method

Two projection functions f and g are used in order to impose the odd symmetry. We have chosen the simplest form, namely

$$f(x) = g(x) = x. \tag{2.33}$$

In order to avoid the short-time approximation the Gaussian nodeless reference function $\varphi_0^{(0)}$ defined in Eq. (2.27) is chosen. Now, using the odd character of the functions $f\varphi_0^{(0)}$ and $g\varphi_0^{(0)}$, the expanded form [Eq. (4.4)] of part I for $I(t)$ reduces to the following form:

$$I(t) = \sum_{k=0}^{+\infty} |\langle n\varphi_0^{(0)} | \varphi_{2k+1} \rangle|^2 e^{-t(E_{2k+1} - E_0^{(0)})}, \tag{2.34}$$

where half of the terms (corresponding to even levels) have disappeared. In fact, due to the numerical nature of the evaluation of $I(t)$, the scalar products $\langle n\varphi_0^{(0)} | \varphi_{2k} \rangle$ could be not exactly zero. Then, residual exponentials associated with even levels may appear with a small amplitude. The numerical experience has shown that such amplitudes were small enough so that no practical trouble results when performing the analysis of $I(t)$. As usual, using the ergodic property we write

$$I(t) = \lim_{T \to +\infty} \frac{1}{T} \int_0^T X^{(0)}(-t/2+\tau) X^{(0)}(t/2+\tau) \times \exp\left[-\int_{-t/2+\tau}^{t/2+\tau} X^{(0)4}(s) ds \right] d\tau. \tag{2.35}$$

Now, an important point related to the numerical evaluation of the quantity above must be pointed out. By using expression (2.27) for $\varphi_0^{(0)}$, we have built a reference diffusion process with a stationary density $p^{(0)}(x) = \varphi_0^{(0)2}$ strongly peaked with a symmetric shape around zero. Accordingly, the trajectory will go through zero very often and the sign of the product $X^{(0)}(-t/2+\tau)X^{(0)}(t/2+\tau)$ will change rapidly. Moreover, the values of the position at two very different times being almost independent (the correlation function of the diffusion process falls exponentially as a function of time) the sign of the previous product will change with a very high rate for large t. The consequence is a large increase of variance in calculations when non small values of t are considered, a situation which contrasts sharply with the one encountered in the calculations for which $f = g = 1$. With such variances for large t, formula (2.22), which requires two large values of t for evaluating E_1, is inadequate, and the Padé-integral transform method for analyzing $I(t)$ becomes essential. We have performed a Padé-z transform analysis of $I(t)$. The results are displayed in Table IV and show a relatively important variance in this approach.

2. Fixed-node (FN) method

In this approach, no problems related to some change of sign as in the expression (2.35) occur since no projection functions are used. The symmetry requirements are directly introduced into the reference function. Here $\varphi_0^{(0)}$ must be odd and is chosen as follows:

$$\varphi_0^{(0)} = x e^{-2^{1/2}/3 |x|^3}. \tag{2.36}$$

Note that in this particular one-dimensional case the node of the exact solution φ_1 is known and consequently the fixed-node procedure actually introduces no approximation.

At this point, it seems important to make a practical remark concerning the use of a variable time step scheme for calculations involving a reference function endowed with nodal hypersurfaces. Let us be more precise. The discretized form of the SDE with $\Delta t \neq 0$ enables us to generate sucessive points on a trajectory through finite jumps but not infinitesimal ones as would be required by the exact continuous SDE. A finite jump may lead the current point to the other side of a nodal hypersurface (through essentially the free diffusion part of the SDE) or very far in a domain of very low probability when the drift vector becomes too large (the "overshooting" effect near the nodes). In order to avoid the important biases associated with these two artificial effects which disappear for really infinitesimal time steps, we used a variable time step scheme. When the magnitude of the drift

TABLE IV. First excited energy E_1 of the quartic oscillator.

I. Simple projection (SP) method [a]	
QMC	2.74(2)
Exact[b]	2.738
II. Fixed-node approach (FNA)[c]	
QMC ($\Delta t = 0.005$)	2.738(4)
Exact[b]	2.738

[a] Calculations have been performed using 1000 trajectories, 20 000 elementary time steps for each trajectory with $\Delta t = 0.1$. A Padé z-transform analysis of $I(t)$ has been done with 30 regularly sampled values $I(t_i)$ with t_i ranging from 0 to 3.

[b] Reference 15.

[c] Calculations have been performed using 100 trajectories, 500 000 elementary time steps for each trajectory. Energy is derived from formula (2.22) with $t_2 = 2.5$ and $t_1 = 2$. Statistical uncertainties are indicated in parentheses.

becomes too important (larger than some threshold value), we take Δt such that the product $|\mathbf{b}|\Delta t$ remains small enough. Thus, the trajectory is slowed down near nodal surfaces and large jumps are avoided. Now, the variance becomes sufficiently low to permit the use of formula (2.22) to obtain E_1.

Results are displayed in Table IV and it clearly appears that the fixed-node (FN) method (Sec. II D 2) actually performs better than the simple projection (SP) method (Sec. II D 1).

E. Harmonic oscillator. Evaluation of the second excited energy E_2

In the previous example illustrating the fixed-node approach, we used a reference function having the right symmetry and the exact node of the solution. Unfortunately, the complete nodal hypersurfaces of exact solutions for more complex systems are generally not known. For atoms or molecules we will use a reference function having the desired symmetry [i.e., belonging to the corresponding irreducible representation of the symmetric group $S(N)$] but *approximate nodes*. At this point, it must be emphasized that, due to the degeneracy of the physical ground state (the "exchange" degeneracy), there is not a single nodal hypersurface associated with the ground state but a (continuous) set of such surfaces. "Approximate" means here that the nodal hypersurface of $\varphi_0^{(0)}$ does not belong to this set. A fixed-node approach with approximate nodes leads to approximate results and in order to remove this approximation the release-node projection (RNP) method presented in part I is examined here. To evaluate the second excited energy of the one-dimensional harmonic oscillator is a simple model problem which gives us the opportunity to introduce in a simple way the main features of this RNP method. In this model problem, the exact solution is known:

$$\varphi_2(x) = (2\pi^{1/2})^{-1/2}(2x^2 - 1)e^{-x^2/2}, \tag{2.37a}$$

$$E_2 = 5/2. \tag{2.37b}$$

1. Fixed-node (FN) method

As a first step, we consider a fixed-node approach where the reference function $\varphi_0^{(0)}$ has the right symmetry (here $\varphi_0^{(0)}$ must be an even function) and approximate nodes. The reference function is chosen as follows:

$$\varphi_0^{(0)}(x) = [2x^2 - (1+d)]e^{-x^2/2}, \tag{2.38}$$

where d is related to the "distance" between approximate nodes and exact ones.

Now, the fixed-node ground-state energy E_2^{FN} can be evaluated for different values of d using, as usual, formula (2.22) and using the variable time step procedure required by the existence of nodes for $\varphi_0^{(0)}$ (see Sec. II D 2 above). Results for $E_2^{\mathrm{FN}}(d)$ are displayed in Table V and illustrate very clearly the existence of the fixed-node approximation. We may notice that the values of $E_2^{\mathrm{FN}}(d)$ lie *below* the exact energy $E_2^{\mathrm{FN}}(0)$. At first sight, this result could appear contradictory with the so-called "variational principle for fixed-node process" considered by Reynolds *et al.*[5] and by Ceperley.[7] The contradiction disappears, however, when we notice that the above variational principle was derived for the following specific situation: (1) to consider the lowest state belonging to some prescribed type of symmetry and (2) to use a reference function belonging to this type of symmetry, so that its nodes are invariant under the corresponding symmetry operations. Failure to fulfill these conditions invalidates the proof. In our present case, assumption (1) is not fulfilled, since the lowest *even* state is E_0 rather than E_2.

2. Release-node projection (RNP) method

Now, we want to remove the fixed-node approximation by using the RNP procedure described in our part I. A nonvanishing third-order polynomial is chosen as "connecting piece" function cpf(x). The reference function is written

$$\varphi_0^{(0)}(x) = |[2x^2 - (1+d)]e^{-x^2/2}| \qquad x \notin (\mp x_n - \epsilon', \mp x_n + \epsilon'), \tag{2.39a}$$

$$\varphi_0^{(0)}(x) = \mathrm{cpf}(x) = A(x \pm x_n)^3 + B(x \pm x_n)^2 + C(x \pm x_n) + D \qquad x \in (\mp x_n - \epsilon', \mp x_n + \epsilon'), \tag{2.39b}$$

where $\pm x_n$ denote the two nodes of the function (2.39a) above. Note that, instead of using a threshold value for the reference function as we did in part I, we directly define here the interval where the connecting piece function is used. Both procedures are essentially equivalent and ϵ' now plays a role similar to that of the quantity ϵ introduced in part I. The coefficients (A, B, C, D) are determined so that the reference function and its first derivative are continuous at the points $\mp x_n - \epsilon'$ and $\mp x_n + \epsilon'$. Expressions of the coefficients (A, B, C, D) in terms of (d, ϵ') are then given as solutions of a linear system of four equations.

As already noticed, φ_2 is not the lowest eigenfunction in the subspace of even symmetry. Consequently the first nonvanishing component of $I(t)$, namely $\langle f\varphi_0^{(0)}|\varphi_0\rangle\langle\varphi_0|g\varphi_0^{(0)}\rangle \times e^{-t(E_0 - E_0^{(0)})}$ could be important enough to trouble the analysis (in particular if large values of t are used) and this situation would require the use of the Padé-integral transform to evaluate E_2. This complication does not occur in the case of atoms or molecules where the true wave function is a lowest state in a given symmetry subspace. Now, in order not to introduce artificial problems in this model problem, we have decided to use functions f and g not only to impose the right symmetry (as it must be in the general case) but also to impose the orthogonality of $f\varphi_0^{(0)}$ and $g\varphi_0^{(0)}$ with φ_0. For that reason we choose

$$f = g = \varphi_2/\varphi_0^{(0)} \tag{2.40}$$

which leads to

$$I(t) = e^{-t(E_2 - E_0^{(0)})}. \tag{2.41}$$

Obviously, in the general case, only the symmetry of the desired state has to be known even if for convenience we have

TABLE V. Harmonic oscillator. Evaluation of E_2.

I. Fixed-node approximation (FNA)[a]	
$d=0.1$	2.346(21)
$d=0.075$	2.401(20)
$d=0.05$	2.451(16)
$d=0.025$	2.484(8)
$d=0$	2.5
II. Release-node projection (RNP)[b]	
$d=0.1 \quad \epsilon'=0.45$	2.49(3)
Exact	2.5

[a] Calculations have been performed using 50 trajectories, 10 000 elementary time steps for each trajectory and $\Delta t=0.001$. Energy is derived from formula (2.22) with $t_2=8$ and $t_1=7.5$.

[b] Calculations have been performed using 50 trajectories, 800 000 elementary time steps for each trajectory and $\Delta t=0.001$. Energy is derived from formula (2.41) with $t=0.4$. Statistical uncertainties are indicated in parentheses.

introduced here its analytical expression through the functions f and g. Now, when ϵ' goes to zero, two phenomena occur. On one hand, since the value of the reference function at the points $\pm x_n$ goes to zero with ϵ', passages from one domain to another one become rare and the variance related to the change of sign of the integrand decreases. On the other hand, $V_p(x)$ in the neighborhood of $\pm x_n$ goes to infinity when ϵ' goes to zero and the sampling of this domain, reponsible for the removal of the nodes, becomes more and more difficult (we try to sample rare events associated with a high value of V_p or, equivalently, we attempt to sample a δ function!). Therefore some compromise has to be found. We present in Fig. 1 the curve giving the variance of calculations versus ϵ'. Clearly an optimal choice for ϵ' may be found in such an approach. The energy for $d=0.1$ is presented in Table V. The difference $E_2^{\mathrm{FN}}-E_2$ being recovered, we conclude that the RNP works for this simple case.

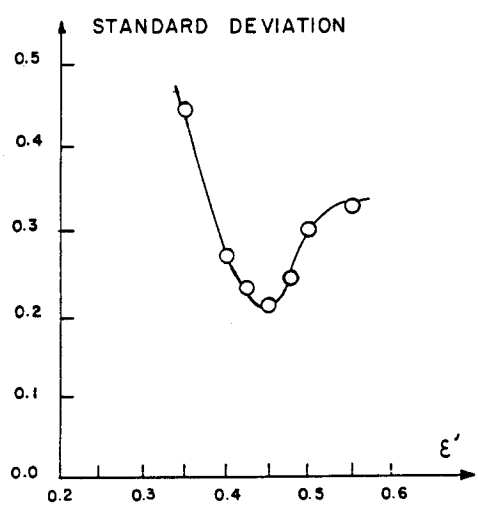

FIG. 1. Standard deviation of the energy as a function of the threshold parameter ϵ' appearing in the RNP method. These values have been obtained for rather short runs. In order to obtain an accurate value of the energy, a 100 times longer run has been performed for the value $\epsilon'=0.45$ which gives the optimal choice of the reference function. The corresponding result is presented in Table V (the standard deviation is actually divided by about $100^{1/2}=10$).

III. SIMPLE ATOMIC AND MOLECULAR SYSTEMS

Molecules are represented in the framework of the Born–Oppenheimer approximation. The potential energy of the molecule is written as

$$V=\sum_{i>j}1/r_{ij}-\sum_{i,\alpha}Z_\alpha/r_{i\alpha}+\sum_{\alpha>\beta}Z_\alpha Z_\beta/r_{\alpha\beta}, \tag{3.1}$$

where $r_{ab}=|\mathbf{r}_a-\mathbf{r}_b|$. Roman indices label electronic coordinates and Greek indices label nuclear coordinates. Z_α is the charge number of nucleus α.

A. Bosonic properties

The purpose of this first subsection is to evaluate energy and observables pertaining to the ground state of two-electron systems. Since no constraints are introduced by the Pauli principle for two-electron systems (see Sec. VI of part I), this ground state is the nodeless mathematical ground state of the Hamiltonian. This is the reason why the properties evaluated in this subsection may be viewed as bosonic properties.

1. Helium-like systems

Before treating helium-like systems, let us give a general expression of a nodeless reference function suitable for an arbitrary atomic system:

$$\varphi_0^{(0)}=\exp\left[\sum_{i,\alpha}a_{i\alpha}r_{i\alpha}+\sum_{i<j}a_{ij}r_{ij}\right]. \tag{3.2}$$

The important point is that this expression includes all the cusp conditions. Note that such a representation has been already discussed in detail in the framework of previous QMC methods (see, e.g., Ref. 5). Obviously, for atomic systems with more than two electrons, this function can be used only in the SP method where a nodeless reference function is needed (see Sec. VI B 2 in part I). The coefficients a_{ab} are chosen in order to reduce as much as possible the perturbing potential V_p. Let us now evaluate the two basic quantities of our algorithm, namely the perturbing potential V_p and the drift vector $\mathbf{b}$. The perturbing potential is evaluated as usual from formula (2.4). After a few algebric manipulations we obtain

$$\begin{aligned}V_p=&\sum_{i>j}1/r_{ij}-\sum_{i,\alpha}Z_\alpha/r_{i\alpha}+\sum_{\alpha>\beta}Z_\alpha Z_\beta/r_{\alpha\beta}\\&-E_0^{(0)}-\sum_{i>j}2a_{ij}/r_{ij}-\sum_{i,\alpha}a_{i\alpha}/r_{i\alpha}\\&-\frac{1}{2}\sum_{\alpha,\beta,i}a_{i\alpha}a_{i\beta}(\nabla_i r_{i\alpha})(\nabla_i r_{i\beta})\\&-\sum_{i,j\neq i,\alpha}a_{ij}a_{i\alpha}(\nabla_i r_{i\alpha})\cdot(\nabla_i r_{ij})\\&-\frac{1}{2}\sum_{i,j\neq i,k\neq i}a_{ij}a_{ik}(\nabla_i r_{ij})\cdot(\nabla_i r_{ik}).\end{aligned} \tag{3.3}$$

Let us introduce the directional vectors

$$\mathbf{u}_{ij}=\tfrac{1}{2}\nabla_i r_{ij}, \tag{3.4a}$$

$$\mathbf{u}_{i\alpha}=-Z_\alpha\nabla_i r_{i\alpha}. \tag{3.4b}$$

Choosing coefficients a_{ij} and $a_{i\alpha}$ such that

$$a_{ij} = a_{ji} = \tfrac{1}{2}, \tag{3.5a}$$

$$a_{k\alpha} = -Z_\alpha, \tag{3.5b}$$

the Coulomb singularities may be entirely suppressed. Finally, we have

$$V_p = \sum_{\alpha>\beta} Z_\alpha Z_\beta / r_{\alpha\beta} - E_0^{(0)} - \frac{1}{2}\sum_{i,\alpha,\beta} \mathbf{u}_{i\alpha}\cdot\mathbf{u}_{i\beta} - \sum_{i,j\neq i,\alpha} \mathbf{u}_{i\alpha}\cdot\mathbf{u}_{ij} - \frac{1}{2}\sum_{i,j\neq i,k\neq i} \mathbf{u}_{ij}\cdot\mathbf{u}_{ik}. \tag{3.6}$$

Now, V_p is a nonsingular bounded function expressed as a sum of bounded scalar products. At this point, it seems appropriate to mention that this result illustrates clearly the necessity of including explicit interelectronic coordinates when a good approximate wave function is wanted. In particular, as noticed by a few authors (see, e.g., Ref. 8), the poor convergence of CI expansions is mainly due to the absence of such r_{ij}-dependent terms in the wave function. Now, a major advantage of all Monte Carlo schemes appears in the possibility of using correlated wave functions without dealing with the complicated integrals that occur in variational methods.

The expression for the drift vector is derived from Eq. (2.13):

$$\mathbf{b} = (\mathbf{b}_1, \mathbf{b}_2, ..., \mathbf{b}_N) \tag{3.7a}$$

with

$$\mathbf{b}_i = \sum_\alpha \mathbf{u}_{i\alpha} + \sum_{j\neq i} \mathbf{u}_{ij}. \tag{3.7b}$$

For two-electron systems, energy and mean value $\langle r_1^2 + r_2^2 \rangle$ have been evaluated using expression (3.2) for the reference function. The constant time step scheme have been used since $\varphi_0^{(0)}$ is nodeless and calculations have been performed for different values of the elementary time step Δt ranging from $\Delta t = 0.02$ to $\Delta t = 0.12$. For each quantity evaluated, a quasiparabolic behavior for the curve representing this quantity vs Δt has been obtained. We therefore systematically performed a least-squares fit to a parabola to determine the extrapolated value at $\Delta t = 0$. We give in Table VI the results concerning the He atom ($Z = 2$) and the Be^{++} ion ($Z = 4$).

As concerns the calculation of the quantity $\langle r_1^2 + r_2^2 \rangle$, the formula (4.7) of part I is written here:

$$\langle \varphi_0 | r_1^2 + r_2^2 | \varphi_0 \rangle = \lim_{t\to+\infty} \frac{\int_{\Omega(-t/2;t/2)} (r_1^2 + r_2^2)[X(t_1)] \exp\left[-\int_{-t/2}^{t/2} V_p[X(s)]ds\right] D^{\varphi_0^{(0)}X} \forall t_1 \epsilon]-t/2, t/2[}{\int_{\Omega(-t/2;t/2)} \exp\left[-\int_{-t/2}^{t/2} V_p[X(s)]ds\right] D^{\varphi_0^{(0)}X}} \tag{3.8}$$

and using the ergodic property this formula may be rewritten as

$$\langle \varphi_0 | r_1^2 + r_2^2 | \varphi_0 \rangle = \lim_{t\to+\infty} \frac{\lim_{T\to+\infty} \frac{1}{T}\int_0^T (r_1^2 + r_2^2)[X^{(0)}(t_1+\tau)] \exp\left[-\int_{-t/2+\tau}^{t/2+\tau} V_p[X^{(0)}(s)]ds\right] d\tau}{\lim_{T\to+\infty} \frac{1}{T}\int_0^T \exp\left[-\int_{-t/2+\tau}^{t/2+\tau} V_p[X^{(0)}(s)]ds\right] d\tau}. \tag{3.9}$$

Results after extrapolation are given in Table VI. It is important to note that E_0 and $\langle r_1^2 + r_2^2 \rangle$ are evaluated simultaneously from the same realization of the process (i.e., from the same set of stochastic trajectories).

2. H_2 molecule

The potential energy of the molecule is

$$V = 1/r_{12} - 1/r_{1A} - 1/r_{1B} - 1/r_{2A} - 1/r_{2B} + 1/R, \tag{3.10}$$

where R is the internuclear distance. Two different reference functions have been used, namely

$$\varphi_0^{(0)} = e^{\frac{\alpha}{2} r_{12}} u(\mathbf{r}_1) u(\mathbf{r}_2) \tag{3.11a}$$

$$\text{with } u(\mathbf{r}_i) = e^{-\xi r_{iA}} + e^{-\xi r_{iB}} \tag{3.11b}$$

and

$$\varphi_0^{(0)} = \exp[-r_{1A} - r_{2B}] + \exp[-r_{2A} - r_{1B}]. \tag{3.12}$$

The first case corresponds to the usual molecular orbital point of view well suited for the equilibrium geometry while the second choice, where $\varphi_0^{(0)}$ is written as a symmetrized product of atomic wave functions, is supposed to be better for large values of R.

In order to illustrate the simplicity of the procedure for evaluating different quantities pertaining to the same eigenstate, we have evaluated from the same basic set of trajectories, not only the energy but also 15 mean values corresponding to multiplicative operators. We have simply chosen the same operators considered by Kolos and Wolniewicz[9] in

TABLE VI. Helium-like systems. Ground state properties.[a]

	He	Be^{++}
	E_0	
SCF	−2.8617	−13.611 3
QMC	−2.903 8(10)	−13.655(11)
"Exact" value	−2.903 72[a]	−13.655 6[b]
	$\langle r_1^2 + r_2^2 \rangle$	
QMC	2.37(2)	0.464(2)
Exact value	2.386 9[c]	0.464 14[d]

[a] Calculations have been performed using 400 trajectories, 40 000 elementary time steps for each trajectory. Energies are derived from formula (2.22) with $t_2 = 10$ and $t_1 = 9$. Mean values are derived from formula (3.9) with $t/2 = 5$ and $t_1 = 0$. Each quantity has been extrapolate to $\Delta t = 0$. All quantities are given in atomic units and statistical uncertainties are indicated in parentheses.
[b] Reference 16.
[c] Reference 17.
[d] Reference 18.

their benchmark calculations concerning the H_2 molecule. In order to appreciate the powerful simplicity of the Monte Carlo approach, it must be pointed out that, for each such observable A, we have just to insert in the program the evaluation of $A[X(t)]$ and to calculate the corresponding accumulator (which, in the present case, amounts merely to inserting in the computer program one single statement per observable!). Calculations have been performed for two values of R corresponding to the two choices of $\varphi_0^{(0)}$. Results are displayed in Table VII, and are very satisfactory.

B. Fermionic properties

In this subsection, the first excited energy E_1 of the helium atom is evaluated. The corresponding eigenstate φ_1 is antisymmetric in the exchange of electron labels and corresponds to the ground state of the antisymmetric representation. In Sec. II D we have shown that the different methods to evaluate properties of the lowest state in a given symmetry subspace do work for simple one-dimensional cases. Here, the aim is to illustrate the validity of those different procedures for atomic and molecular systems.

1. Simple projection (SP) method

We choose

$$\varphi_0^{(0)} = \exp[-2r_1 - 2r_2 + \tfrac{1}{2}r_{12}] \tag{3.13}$$

and

$$f = g = \tfrac{1}{4}[(1-r_1)e^{r_1} - (1-r_2)e^{r_2}]. \tag{3.14}$$

TABLE VII. H_2 molecule. Ground state properties.[a]

	$R=1.4$[c]		$R=4$[d]	
	QMC	Exact[b]	QMC	Exact[b]
E_0	−1.175(1.7)	−1.1745	−1.0167(7)	−1.016 37
$\langle r_{12}^{-1}\rangle$	0.587(2.6)	0.5874	0.263(1.5)	0.263 0
$\langle r_{12}\rangle$	2.169(9)	2.1690	4.33(1.5)	4.327
$\langle r_{12}^2\rangle$	5.63(4.5)	5.632	20.6(1.3)	20.569
$\langle r_A\rangle$	1.550(6)	1.5499	2.86(1.3)	2.863
$\langle r_A^{-1}\rangle$	0.908(4)	0.9128	0.610(3.5)	0.613 6
$\langle r_A^2\rangle$	3.04(2)	3.036	10.79(8.5)	10.815
$\langle r_A r_B\rangle$	2.71(2)	2.704	6.68(2.3)	6.663
$\langle r_{1A} r_{2A}\rangle$	2.33(1.5)	2.321	6.57(3)	6.551
$\langle r_{1A} r_{2B}\rangle$	2.39(1.5)	2.385	9.82(3)	9.806
$\langle z_1 z_2\rangle$	−0.156(5.5)	−0.1596	−3.39(6)	−3.392
$\langle x_1 x_2\rangle$	−0.055(3.5)	−0.0551	−0.039(4.5)	−0.038 4
$\langle z^2\rangle$	1.02(2)	1.023	4.74(4)	4.708
$\langle x^2\rangle$	0.76(2)	0.762	1.05(1.5)	1.054
$\langle r^2\rangle$	2.55(4)	2.546	6.85(5.5)	6.815
Q	0.9(1)	0.91	1.3(1.5)	1.38

[a] Calculations have been performed using 50 trajectories and about 10^6 elementary time steps for each trajectory with $\Delta t = 0.01$. Energies are derived from formula (2.22) with $t_2 = 20$ and $t_1 = 19$. Each mean value is derived from formula (4.7) of part I with $t/2 = 10$ and $t_1 = 0$. Q denotes the electric quadrupole moment of the molecule defined as $Q = R^2 - 2(3\langle z^2\rangle - \langle r^2\rangle)$. All quantities are given in atomic units and statistical uncertainties are indicated in parentheses.

[b] Reference 9.

[c] Using Eq. (3.11) for $\varphi_0^{(0)}$ with $\alpha = 0.56$ and $\xi = 1.285$.

[d] Using Eq. (3.12) for $\varphi_0^{(0)}$.

As it must be, $f\varphi_0^{(0)}$ and $g\varphi_0^{(0)}$ are antisymmetric in the exchange of electron labels. Moreover, by using the atomic orbital model, f and g have been choosen such that $f\varphi_0^{(0)}$ and $g\varphi_0^{(0)}$ have a maximum overlap with φ_1. This last point simplifies the analysis of $I(t)$ as sum of real exponentials by giving an important weight to the first nonvanishing exponential associated with E_1.

As already noticed in Sec. II D 1, the nonconstant sign of f and g prevents any attempt to use formula (2.22) for calculating E_1. Thus a Padé-z transform analysis must be performed. A very predominant real exponential associated with E_1 appeared and then the first Padé approximant[6] was sufficient to extract E_1. The results are displayed in Table VIII.

2. Fixed-node (FN) approach

In this case, the complete nodal hypersurface of φ_1 is known (its equation is $r_1 = r_2$).[10,11] However, even if there is no fixed-node approximation here, the aim is to verify that our scheme works for atomic systems.

The following reference function is chosen:

$$\varphi_0^{(0)} = (1-r_1)e^{-r_1}e^{-2r_2} - (1-r_2)e^{-r_2}e^{-2r_1} \tag{3.15}$$

and the same algorithm as in Sec. II D 2 is used. Conclusions are identical with those obtained in this previous case: due to the constant sign of the integrand, the variance is markedly smaller than in the previous (SP) method, and formula (2.22) for evaluating the energy may be used. The variable time step procedure permits to avoid undesirable effects. Results are displayed in Table VIII.

IV. CONCLUSIONS

While part I of the present work was devoted to the theoretical description of our Monte Carlo method, the purpose of the present part II was to consider with some detail the various practical and numerical aspects pertaining to its computer implementation.

It appeared convenient to organize the discussion around three main points:

(1) The convergence problem (time-length of each

TABLE VIII. First excited energy E_1 of the helium atom (triplet state).

I. Simple projection (SP) method[a]	
QMC	−2.175(10)
Exact[b]	−2.1752
II. Fixed-node (FN) method[c]	
QMC	−2.175(3)
Exact[b]	−2.1752

[a] Calculations have been performed using 400 trajectories, 15 000 elementary time steps for each trajectory. A Padé z-transform analysis of $I(t)$ has been done with about 30 regularly sampled values $I(t_i)$ with t_i ranging from 0 to about 3. Four calculations with $\Delta t = 0.04$, 0.03, 0.02, and 0.01 have been done and a least-squares fitting to a parabola was performed to extrapolate to $\Delta t = 0$.

[b] Reference 17.

[c] Calculations have been performed using 50 trajectories, 100 000 elementary time steps for each trajectory with $\Delta t = 0.01$. Energy is derived from formula (2.22) with $t_2 = 40$ and $t_1 = 36$. Statistical uncertainties are indicated in parentheses.

sample trajectory, number of such trajectories, choice of the reference function $\varphi_0^{(0)}$).

(2) The sources of systematic biases: the quality of the random number generator, the time-discretization error in the generation of the sample trajectories (the so-called "short-time approximation") and the time-discretization error pertaining to the evaluation through a finite Riemann sum of the integral appearing as the exponent in the Feynman–Kac factor [see, e.g., Eq. (3.7) of part I].

(3) The specific problems related to the problem of obtaining states belonging to some prescribed symmetry, the most important case corresponding to the Pauli principle requirements in many-fermion systems.

We have first treated a number of one-dimensional examples [involving harmonic (x^2) and quartic (x^4) potentials] in order to illustrate the various points listed above and to propose some solutions when necessary. As a conclusion of this first step, we found it is possible to keep under control all the above listed sources of error. Second, with the purpose of moving towards the study of more interesting physical systems, we considered the simplest (two-electron) atomic and molecular systems, namely helium-like systems (He, Be^{++}) and hydrogen molecule. For these systems, our results are of comparable quality with those obtained within the framework of the other QMC methods (see, e.g., Refs. 5 and 12–14). We did not content ourselves with the (bosonic) ground state energy, since this would not at all be a typical representative for many-electron atomic and molecular systems, where the Pauli principle becomes really involved: we also considered the lowest triplet state (antisymmetric space function) as a model of the symmetry requirements to be taken into account for these larger systems. On the other hand, we also evaluated a number of observables other than the energy, in order to illustrate how easily such evaluations can be performed in the framework of the present Monte Carlo method.

As concerns the perspectives for future developments, two steps may appropriately be distinguished. A first step would rely (as many previous Monte Carlo computations did) on the fixed-node approximation for evaluating energy and observables (including now, response properties). According to the experience borrowed from other QMC computations, we may expect that such calculations could be achieved with reasonable accuracy for systems having a number of electrons ranging up to about ten. The second step, would consist in applying to many-electron systems the release-node projection (RNP) method, the results of which appeared rather encouraging for the one-dimensional system to which it was applied in the present work. Investigation concerning these two steps is presently in progress.

ACKNOWLEDGMENTS

We would like to thank the "Conseil Scientifique du Centre de Calcul Vectoriel pour la Recherche" for providing us with computer facilities from which the major part of previous calculations have been done. We are also indebted to the "Centre Inter Régional de Calcul Electronique" (CIRCE) for allowing us to make use of facilities on NAS 9080 and IBM 3090/200 computers and to the "Centre de Calcul Recherche (Paris VI)" for facilities on its GOULD PN9050.

[1] M. Caffarel and P. Claverie, J. Chem Phys. **88**, 1088 (1988), referred to as part I.
[2] J. Vrbik and S. M. Rothstein, J. Comp. Phys. **63**, 130 (1986).
[3] H. Risken, *The Fokker–Planck Equation* (Springer, Berlin, 1984).
[4] H. Cramér, *Mathematical Methods of Statistics* (Princeton University, Princeton, 1966), Chap. 8.2.
[5] P. J. Reynolds, D. M. Ceperley, B. J. Alder, and W. A. Lester, Jr., J. Chem. Phys. **77**, 5593 (1982).
[6] (a) E. Yeramian and P. Claverie, Nature **326**, 169 (1987); (b) P. Claverie, A. Denis, and E. Yeramian, Comp. Phys. Rep. (submitted); (c) J. Aubard, P. Levoir, A. Denis, and P. Claverie, Comp. Chem. **11**, 163 (1987).
[7] D. M. Ceperley, in *Recent Progress in Many-Body Theories*, edited by J. Zabolitzky, M. de Llano, M. Fortes, and J. W. Clark (Springer, Berlin, 1981), pp. 262–269.
[8] W. Kutzelnigg, Theor. Chim. Acta **68**, 445 (1985).
[9] W. Kolos and L. Wolniewicz, J. Chem. Phys. **43**, 2429 (1965).
[10] D. J. Klein and H. M. Pickett, J. Chem. Phys. **64**, 4811 (1976).
[11] M. D. Kostin and K. Steighitz, Phys. Rev. **159**, 27 (1967).
[12] J. B. Anderson, J. Chem. Phys. **73**, 3897 (1980).
[13] J. B. Anderson, J. Chem. Phys. **65**, 4121 (1976).
[14] J. B. Anderson, Int. J. Quantum Chem. **15**, 109 (1979).
[15] F. T. Hioe, D. MacMillen, and E. W. Montroll, Phys. Rep. **43**, 305 (1978).
[16] K. Frankowski and C. L. Pekeris, Phys. Rev. **146**, 46 (1966).
[17] C. L. Pekeris, Phys. Rev. **115**, 1216 (1959).
[18] W. A. Sanders and J. O. Hirschfelder, J. Chem. Phys. **42**, 2904 (1965).